



Sorption studies for the removal of arsenite onto *Pinus roxburghii* cone: pH, isothermal, kinetics and thermodynamic studies

Naseem Rauf^{a,*}, Guangliang Liu^a, Yong Cai^a, S.S. Tahir^b

^aDepartment of Chemistry, Southeast Environmental Research Center, Florida International University, Miami, FL 33199, USA, Tel. +1 305-348-6235; emails: naseemrauf@yahoo.com (N. Rauf), liug@fiu.edu (G. Liu), Tel. +1 305-348-6210; email: cai@fiu.edu (Y. Cai)

^bEnvironmental Analytical Laboratory, National Physical and Standards Laboratory (NPSL), 16, H-9, Islamabad, Pakistan, Tel. +92-51-9225387; email: dtpcsir@yahoo.com

Received 4 November 2014; Accepted 25 December 2019

ABSTRACT

In this study, *Pinus roxburghii* cones were used for the removal of arsenite from aqueous solutions. Activated carbon was prepared from these cones with further activation of it with H_3PO_4 (1:1), KOH (1:3) and 0.5 M $FeSO_4$. Preliminary experiments show that no significant removal of arsenite took place by using raw carbon and its activation with H_3PO_4 and KOH while activated carbon modified with 0.5 M $FeSO_4$ gives maximum removal of arsenite (99%). So further experiments were carried out by using activated carbon with 0.5 M $FeSO_4$ (Fe-GAC). Its surface properties were investigated in terms of surface area, particle size, moisture, ash contents, cation exchange capacity, pH_{PZC} and elemental analysis through. The removal experiments of arsenite were carried out by the sorption technique in a batch system. Competitive sorption of arsenite in the presence of various metals like V, Cr, Co, Cu, Se, Cd, Ba, Tl, Be, Pb, and Ni was also investigated with an adsorbent dosage range of 0.2–1.5 g. Hydride generation-atomic fluorescence spectrometry and inductively coupled plasma-mass spectrometry technique was used for the analysis of arsenite and other metals in aqueous solutions. The adsorption of arsenite was pH-dependent. The kinetics of adsorption was examined in terms of the pseudo-first-order and pseudo-second-order. The adsorption data were applied to the well-known Langmuir, Freundlich, and Temkin isotherm models. Thermodynamic parameters (ΔH° , ΔS° , and ΔG°) were calculated from the slope and intercept of plots of $\ln K_D$ vs. $1/T$ at different temperatures of 298, 313 and 323 K.

Keywords: *Pinus roxburghii*; Sorption; Isotherms; Kinetics; Thermodynamics; Arsenite

1. Introduction

Arsenic is a natural component of the earth's crust and is widely distributed throughout the environment in the air, water, and land in both inorganic and organic forms. However, inorganic arsenic is considered to be the most toxic form of the element as the organic arsenic detoxifies through methylation [1]. Naturally occurring inorganic arsenic is stable in oxidation states of –III as in arsine gas (AsH_3), 0 as in crystalline arsenic, +III as in arsenite, and +V as in arsenate. In the relatively pristine natural groundwater

environment, arsenic(III) and arsenic(V) are typically the dominant forms of arsenic. Among these As(III) is more toxic than As(V) [2].

Chronic exposure to low levels of arsenic has long been linked to adverse health effects in humans. Long-term exposure to arsenic can cause bladder, lungs, skin, kidney, liver, and prostate cancer [3]. Considering the high toxicity of arsenic, the World Health Organization (WHO) and the U.S. Environmental Protection Agency set the maximum acceptable level of arsenic in drinking water at 10 $\mu\text{g/L}$ [4,5].

Various techniques reported for the removal of arsenic included precipitation [6], reverse osmosis [7], pre-oxidation

* Corresponding author.

processes [8] and ion-exchange [9]. However, disadvantages associated with precipitation include higher operating and chemical costs, and the formation of by-products [10] requiring large containment and settling beds, as well as the handling and final disposal of the contaminant-laden sludge, which can be expensive. Disadvantages with membrane process including high operating costs, the high cost of membrane replacement, the need for pretreatments of the influent to prevent membrane fouling, and handling and disposal of the toxic-laden waste can make these systems expensive and impractical [9,10]. In reverse osmosis, as with other arsenic removal methods, pretreatment may be necessary to prevent fouling of the ion exchange resin [7].

Among various remediation technologies, adsorption is considered as one of the more effective and efficient ways for the removal of arsenic from water. In recent years activated carbons prove to be very efficient adsorbent for the removal of toxics from water and wastewater due to its high surface area and porosity. However, the cost associated with the production and import of it is relatively very high for developing countries. In the past few years, production of activated carbon-based on biomass from agriculture waste/by-products has gained significant importance and can be used as cheap and effective sorbents in their natural as well as physically or chemically modified forms such as olive stones [11], coconut shell [12–14], pine sawdust [15], almond and pecan shells [16], eucalyptus wood chars [17], peanut hulls [18] and oat hulls [19] has been used successfully in the preparation of activated carbons.

Pinecone derived activated carbon was used previously for the removal of methyl orange [20], congo red [21], lead [22], remazol brilliant blue R [23], methylene blue [24], phenol, and Cr-VI [25]. The use of surface-modified adsorbents has to gain particular attention in the last few years. Previously the potential of a raw pine cone and its modified form with zinc loading was evaluated for the removal of As(III) from the aqueous solution [26]. Iron oxides, oxyhydroxides, and hydroxides, including amorphous hydrous ferric oxide (FeO–H), goethite (–FeO–OH) and hematite (–Fe₂O₃), are promising adsorbents for removing both arsenite and arsenate from the water. However, most iron oxides are fine powders that are difficult to separate from the solution after adsorption. Adsorption onto iron-tailored activated carbon is considered to be one of the most promising technologies because it is economical and easy to set up, and because the skeletal structure of the activated carbon is strong, whereas granular iron media are fragile.

Our aim was to develop an adsorbent from the cones of *Pinus roxburghii* that is cheaper, simple and environmentally friendly and then its activation onto its active sites in such a manner that much of the arsenite can be removed on to this adsorbent. The finding of this study can be useful in the development of economical and easy to use treatment system for arsenic from drinking water, especially in developing countries.

2. Experimental procedure

2.1. Preparation of activated carbon from *Pinus roxburghii*

The cones of *Pinus roxburghii* were collected around the Margalla Hills from the city of Islamabad, Pakistan.

These were brought into the laboratory and were washed several times with distilled water to remove any dust and surface impurities and were dried in the air for several days. These were heated in an electric oven for 60 min at 448 K. After cooling, the burned cones were crushed into powdered form to get a uniform particle size and were then stored in an airtight container.

For chemical activation, a known quantity of the stored raw carbon was mixed with H₃PO₄ (H-GAC) in the impregnation ratio of 1:1. It was kept in an oven at 423 K for 48 h. After impregnation, the sample was washed with distilled water until there was no change in its pH. The washed activated carbon was dried at 383 K for 2 h in an electric oven and was stored in desiccators for further use. In another process of activation, raw carbon was impregnated with KOH (K-GAC) in the ratio of 1:3 and was heated at 343 K for until the remaining solution evaporated. The sample was washed several times with distilled water until there was no change in pH. For iron loading, FeSO₄ was used instead of FeCl₃ due to better intraparticle diffusion of Fe(II) as compared to Fe(III). It has been reported earlier that Fe(III) can easily hydrolyze to form large metal particle clusters which cannot diffuse easily into the internal pores of the activated carbon due to its precipitation. For iron loading, 10.0 g of the raw carbon was placed in 125 mL Nalgene bottles with 50 mL of 0.5 M FeSO₄. It was shaken on a reciprocating shaker at 125 rpm for 48 h at constant temperature (298 ± 1 K). Following the decanting of the supernatant, solids were washed with distilled water until there was no detection of greenish color in the filtrate and no detection of sulfate [27]. The washed activated carbon was then dried at 383 K for 2 h in an electric oven and was stored in a desiccator for further use. The schematic diagram of the preparation of activated carbon from pinus cones and its activation is illustrated in Fig. 1.

2.2. Characterization of iron loaded activated carbon (Fe-GAC)

The Fe-GAC was characterized for pH, moisture content, ash, cation exchange capacity (CEC), pH_{PZC}, surface area, particle size, and elemental analysis. The CEC was determined by the BaCl₂ compulsive exchange method [28]. pH, moisture, CEC, ash, and pH_{PZC} were determined by the methods reported by Shrestha et al. [29]. The specific surface area of Fe-GAC was estimated using Sears' method [30]. Elemental analysis for C, H, N, and S was performed on a CHNS Analyzer (Elementar Vario EL III). X-ray diffraction (XRD) measurement of the Fe-GAC was made by using CuK_α radiation (40 KV, 30 mA) over the 2θ range of 10°–70° onto PANalytical X'Pert PRO XRD spectrometer by using powder diffraction procedure. The Brunauer–Emmett–Teller (BET) surface area of the activated carbon was measured using a BET Quantasorb Sorption System, Model No. QS-11.

2.3. Preparation of arsenite solutions and its estimation by atomic fluorescence spectrometry

All of the reagents and chemicals used were of analytical grade and solutions were prepared by using Milli-Q water (Barnstead Nanopure Diamond with a resistivity of 18.2 MΩ cm). NaAsO₂ was purchased from Sigma-Aldrich

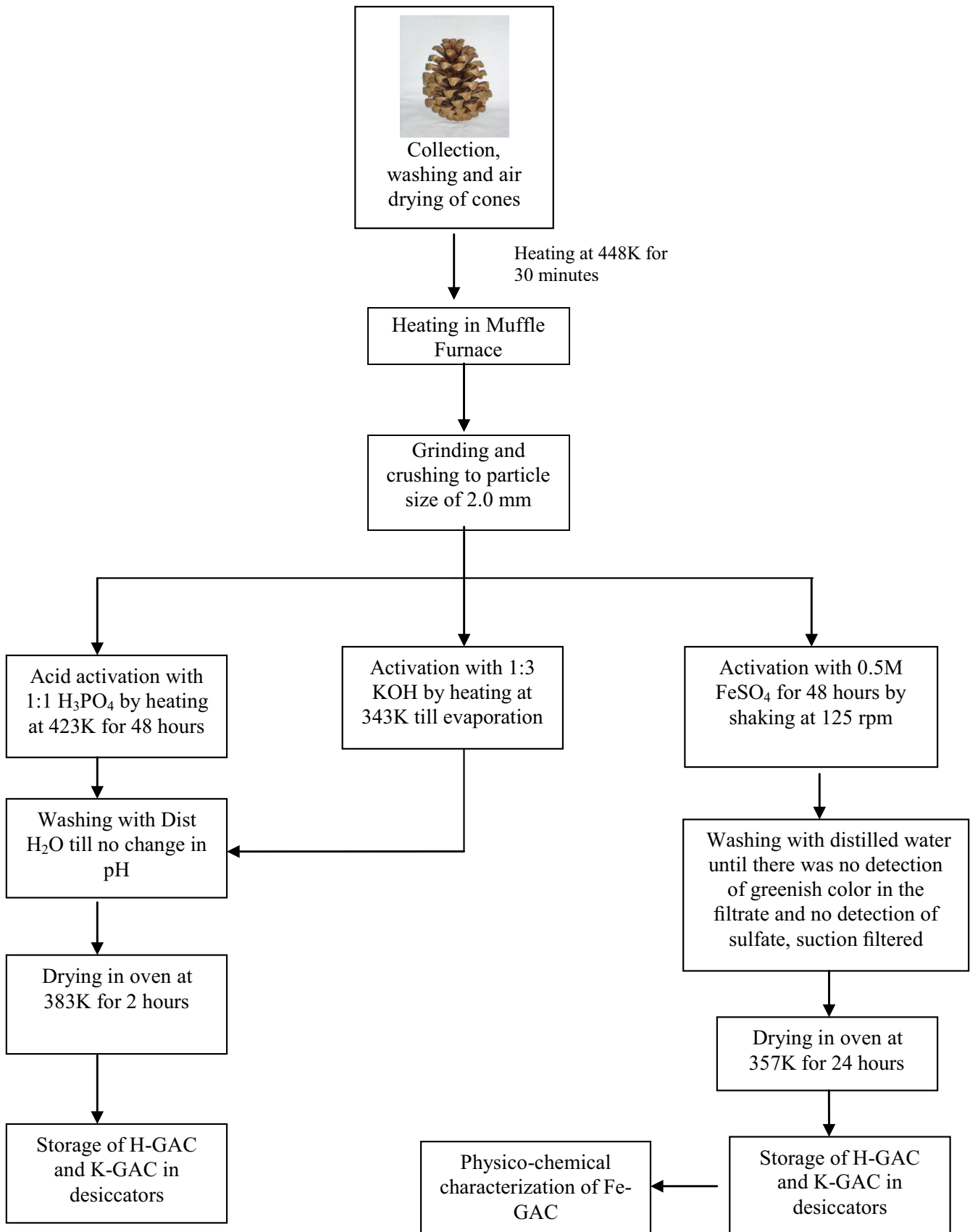


Fig. 1. Schematic diagram for the preparation of activated carbon from the cones of *Pinus roxburghii*.

having a purity of 98%. A stock solution of 1,000 mg/L of arsenite was prepared by dissolving accurately weighed the amount of NaAsO_2 in 5% HNO_3 and kept at 4°C. The experimental solutions were obtained by diluting the stock solution in accurate proportions to the desired initial concentrations. The concentration of arsenite was measured by using hydride generation-atomic fluorescence spectrophotometer (HG-AFS) (P S Analytical, PSA 10.055 Millennium Excalibur) and inductively coupled plasma coupled with mass spectrophotometer (ICP-MS) (Perkin-Elmer ELAN, DRC-e). The other instrumental and experimental conditions used are given in Table 1.

2.4. Sorption experiments

Sorption measurements were made in triplicate by the batch technique at room temperature (298 ± 2 K) except where specified. The percent removal and sorption capacity of arsenite were calculated as done previously [31]. For kinetic studies of arsenite onto Fe-GAC, solutions containing 100 $\mu\text{g/L}$ of As(III) were separately shaken with 1.0 g of the adsorbent for different time intervals ranging from 5 to 120 min. The temperature studies were carried out at different concentrations of 150, 200, 250 and 300 $\mu\text{g/L}$ of arsenite at 298, 313 and 323 K and were separately shaken with 1.2 g of Fe-GAC for 1 h. The experiment for the effect of pH on the adsorption was carried out at pH values ranging from 2.6–12 and was controlled by the addition of dilute HCl/NaOH solutions. The pH of the solution was measured with a pH meter (Fischer Scientific AR-15). For pH determination of the solutions, the pH meter was calibrated every time with buffers of pH 4.0 and 10.0. Isothermal studies of arsenite were conducted with an adsorbent quantity of 1.2 g having

arsenite concentrations in the range of 100–350 $\mu\text{g/L}$ in identical conical flasks. A blank was maintained to determine the effect of arsenite sorption on the conical flasks. After the addition of adsorbent (Fe-GAC), the reaction mixtures were agitated in the shaker at 200 rpm for 1 h (estimated equilibrium time) at different temperatures of 298, 313 and 323 K.

The samples were withdrawn from the flasks and adsorbent was separated from the solution by centrifugation at 10,000 rpm for 10 min. The samples were diluted with 30% HCl and 2% HNO_3 before analysis by using HG-AFS and ICP-MS respectively in order to achieve results in the desired calibration range of 5–50 $\mu\text{g/L}$ of As(III) standards.

2.5. Arsenite sorption in presence of various metal ions

Competitive sorption experiment of arsenite was conducted in the presence of various metal ions. For this purpose metals like V, Cr, Co, Cu, Se, Cd, Ba, Tl, Be, Pb, and Ni having a concentration of 100 $\mu\text{g/L}$ each was shaken with the already optimized conditions for arsenite, that is 1.2 g of Fe-GAC for 1 h. After 1 h of equilibration time, the concentration of arsenite and other metals in the supernatant was measured by using an ICP-MS (Perkin-Elmer ELAN, DRC-e) and the sorption capacity was calculated.

3. Results and discussion

3.1. Characterization of FeSO_4 modified activated carbon obtained from *Pinus roxburghii* cones

Four series of activated carbon was prepared from the cones of *Pinus roxburghii*. These include the raw carbon simply obtained by heating and the other three by chemical

Table 1
Instrumental and chemical conditions for arsenic and other metals using hydride generation-atomic fluorescence spectrophotometer (HG-AFS) and inductively coupled plasma-mass spectrophotometer (ICP-MS)

| HG-AFS | |
|---|--|
| Reagent blank | 30% v/v HCl, 50% KI, 10% ascorbic acid |
| Reductant | 0.7% m/v sodium borohydride (NaBH_4) in 0.1 mol/L sodium hydroxide (NaOH) |
| Sample | 30% v/v HCl, 50% KI, 10% ascorbic acid |
| Carrier gas, argon (gas–liquid separator) | 300 ml/min of flow rate |
| Nitrogen (dryer gas) | 2.5 L/min of flow rate |
| Reductant (NaBH_4) flow rate | 4.5 ml/min |
| Sample flow rate | 9.0 ml/min |
| Primary current | 27.5 mA |
| Boost current | 35.0 mA |
| ICP-MS | |
| Sample | 2% HNO_3 , 40 μL of Yttrium (40 ppb) |
| Standard | 2% HNO_3 , 20 μL of Yttrium (20 ppb) |
| Blank | 2% HNO_3 , 40 μL of Yttrium (40 ppb) |
| Plasma gas flow | 14 L/min |
| Nebulizer gas flow | 0.89 L/min |
| Auxilliary gas flow | 1.2 L/min |
| Sample uptake rate | 40.0 rpm |
| RF power | 1,400 W |

activation with KOH, H_3PO_4 , and $FeSO_4$. $FeSO_4$ treated carbon was characterized in terms of specific and BET surface area, particle size, ash content, moisture, pH, and other parameters reported in Table 2. The prepared GAC exhibited low moisture content of 2.1% (Table 2). Generally, the recommended moisture content for the storage of activated carbon is less than 3% [32] as higher moisture content can lower the storage and shelf-life of activated carbon due to more susceptibility to fungal growth. Its ash contents were 3.78%. In general, the percentage of ash in a commercial activated carbon is higher than 10% [33]. The ash content is directly related to the pH of GAC and the measured pH value was 4.77.

CEC is about the relative number of negatively charged binding sites on the surfaces of a substance attracting and binding positively charged ions. The CEC was 2.78 meq/g. The reported value of CEC in literature is 2.42 and 2.33 for activated carbon prepared from Olive-waste cakes and coconut shell respectively [34,35]. The specific surface area pH_{pzc} determined was 999 m^2/g and 2.6 respectively. Activated carbons are usually classified as powdered activated carbons (PAC) with fine granules whose size is less than 1.0 mm, granulated activated carbon (GAC) whose size is between 0.425–2.36 mm. The activated carbon produced was GAC with a particle size of 2.0 mm. PAC is not generally used for adsorption purposes because of their high-pressure loss in applications and also PAC requires subsequent separation by coagulation/sedimentation/filtration and regeneration is difficult. Granular activated carbon is used for deodorization, water treatment and separation of components in a flow system and can also be used for gas/vapor phase applications. GAC requires less carbon, no subsequent separation is needed, beds are easier to monitor with respect to performance and can be regenerated. Elemental analysis on CHNS shows that it contains 57.59% of carbon as the major constituent of it.

Fig. 2 represents the XRD pattern of the raw and the activated carbon-supported $FeSO_4$. Fig. 2a presents the XRD pattern with peak at $2\theta = 21^\circ\text{--}23^\circ$, which can be ascribed to the amorphous morphology of the activated carbon heated

at 423 K, while the XRD pattern of the activated carbon impregnated with $FeSO_4$ (Fe-GAC, Fig. 2b) shows a number of sharp peaks which are compatible with the presence of activated carbon impregnated with $FeSO_4$.

3.2. Arsenite removal onto raw, H_3PO_4 , KOH and $FeSO_4$ treated carbon obtained from *Pinus roxburghii* cones

The removal of arsenite onto raw, H_3PO_4 , KOH and $FeSO_4$ treated carbon is shown in Fig. 3. The results show that the maximum removal of arsenite, that is >70% has been achieved by using activated carbon modified with $FeSO_4$ with 1.0 g of dosage while it was 19.51%, 17.60%, and 23.78% by using H_3PO_4 , KOH, and raw carbon respectively. The removal of arsenite was in the order of Fe-GAC > Raw carbon > H_3PO_4 > KOH. Keeping in view the higher efficiency of Fe-GAC for arsenite removal, further experiments were carried out by using Fe-GAC.

3.3. Adsorption isotherms

In the present studies, equilibrium sorption data of arsenite onto Fe-GAC was applied to three well known and widely applicable different isotherm equation namely Langmuir, Freundlich, and Temkin.

The Langmuir adsorption isotherm describes quantitatively the buildup of a layer of molecules on an adsorbent surface as a function of the concentration of the adsorbed material in the liquid in which it is in contact. In a modified form it can also describe a bi-layer deposition.

The linear form of the Langmuir isotherm equation is represented in the equation [36].

$$\frac{C_e}{q} = \frac{1}{bX_m} + \frac{C_e}{X_m} \quad (1)$$

X_m and b are the Langmuir constants related to adsorption capacity and energy of adsorption. The values of X_m (mg/g) and b (dm^3/mg) were calculated from slope and intercept of the linear plots of C_e/q vs. C_e respectively (Fig. 4). The values of X_m (mg/g) and b (dm^3/mg) are shown in Table 3 for arsenite at different temperatures of 298, 313 and 323 K.

To determine if the adsorption process is favorable or unfavorable, for the Langmuir-type adsorption process, the isotherm shape can be classified by the term ' R_L ' a dimensionless constant separation factor, which is defined as below [37].

$$R_L = \frac{1}{(1 + bC_0)} \quad (2)$$

where R_L is a dimensionless separation factor, C_0 is initial arsenite concentration (mg/dm^3) and b is Langmuir constant (dm^3/mg). The isotherm is unfavorable when $R_L > 1$, the isotherm is linear when $R_L = 1$, the isotherm is favorable when $0 < R_L < 1$ and the isotherm is irreversible when $R_L = 0$. The values of R_L for adsorption of arsenite onto Fe-GAC at studied different concentrations were between 0 and 1 (Table 3), which indicates favorable adsorption.

Table 2
Physico-chemical characteristics of Fe-GAC

| Parameter | Value |
|---|-------|
| pH | 4.77 |
| pH_{pzc} | 2.6 |
| Cation exchange capacity (CEC), (meq/g) | 2.78 |
| Moisture content (%) | 2.1 |
| Ash (%) | 3.78 |
| Particle size (mm) | 2.0 |
| Specific surface area (m^2/g) | 999 |
| BET surface area (m^2/g) | 1,122 |
| CHNS analysis | |
| Carbon as C (%) | 57.59 |
| Nitrogen as N (%) | 0.50 |
| Sulphur as S (%) | 0.83 |
| Hydrogen as H (%) | 2.75 |

Another common isotherm model is the Freundlich, which is suitable for use with heterogeneous surfaces but can describe adsorption data over a restricted range only [38]. It can be written in a linear form as:

$$\log(q) = \log K + \left(\frac{1}{n}\right) \log C_e \quad (3)$$

by plotting $\log q$ against $\log C_e$, the slope is $1/n$ and intercept are $\log K$ (Fig. 5). The Freundlich constant, $1/n$ ranging between 0 and 1 is a measure of adsorption intensity or surface heterogeneity, becoming more heterogeneous as its value gets closer to zero. Values of K and $1/n$ are provided in Table 3.

Temkin and Pyzhev [39] considered the effects of some indirect adsorbate/adsorbate interactions on adsorption isotherms. They suggested that, because of these interactions and ignoring very low and very large values of concentration, the heat of adsorption of all molecules in the layer

would decrease linearly with coverage. The derivation of the Temkin isotherm assumes that the fall in the heat of sorption is linear rather than logarithmic, as implied by the Freundlich equation. The Temkin isotherm has generally been applied in the following form:

$$q_e = B \ln A + B \ln C_e \quad (4)$$

where $B = (RT/b)$, q_e (mg/g) and C_e (mg/dm³) are the amounts adsorbed at equilibrium and the equilibrium concentration, respectively. Also, T the absolute temperature in K and R is the universal gas constant, 8.3143 J/mol K . The constant b is related to the heat of adsorption. A and B are constants related to adsorption capacity and intensity of adsorption. Plots of $\ln C_e$ against q_e are given in Fig. 6 and the constants A and B are listed in Table 3.

Examination of the linear isotherm plots suggested that the Langmuir model yielded a much better fit than the other isotherm models. Overall, the Langmuir isotherm has

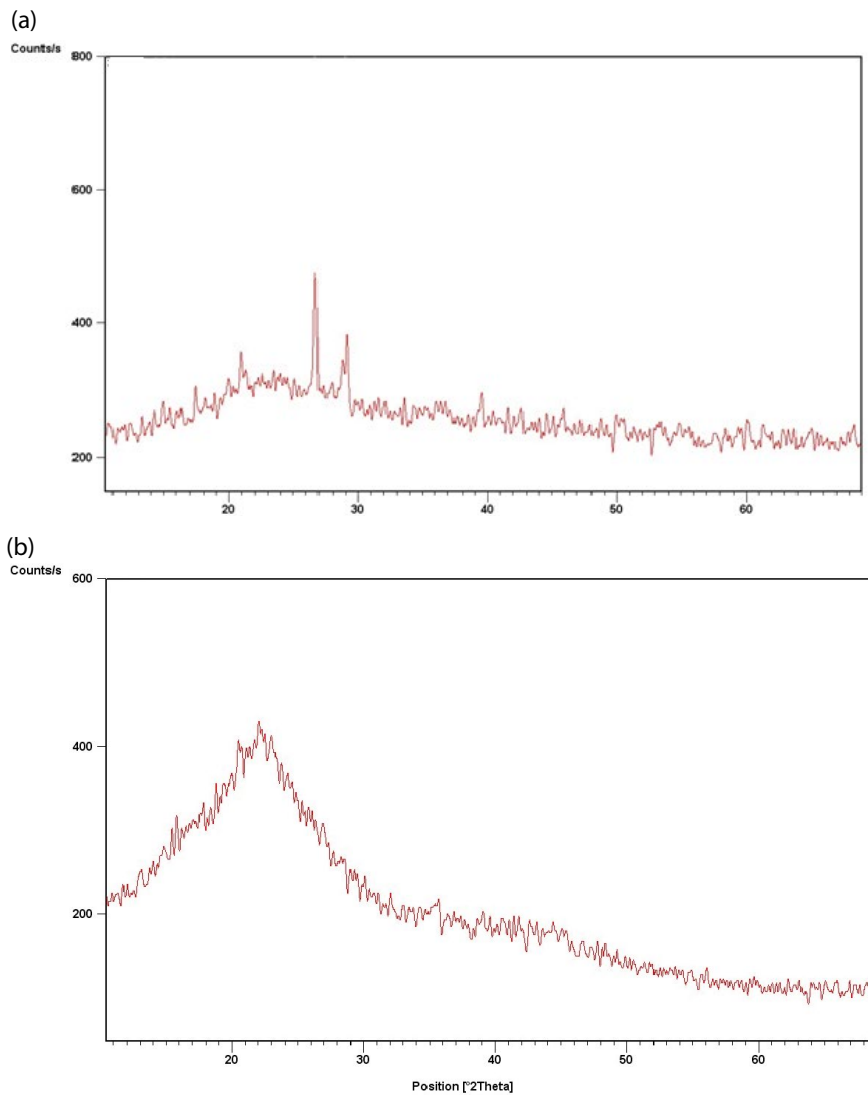


Fig. 2. XRD pattern of the raw and the activated carbon-supported FeSO₄.

the highest R^2 values (0.999), whereas the Freundlich and Temkin values are lower. So, the linearized forms of the Langmuir isotherms are found to be linear over the whole concentration range studied, and the correlation coefficients were extremely high, confirming the monolayer coverage of arsenite onto particles and also the homogenous distribution of active sites on the material since the model presupposes that the surface is homogenous. The X_m values also showed that the adsorption capacity decreased with increasing temperature (Table 3), may be due to weak adsorption interaction between Fe-GAC surface and the arsenite, which supports physisorption. At high temperature, the thickness of the boundary layer decreases, due to the increased tendency of the metal ion to escape from the activated carbon surface to the solution phase, which results in a decrease in adsorption as temperature increases. The same type of behavior has been reported previously, where the adsorption of As(III) onto thioglycolate sugarcane carbon decreased with increasing temperature from 35°C to 45°C [40].

The adsorption capacities of various activated carbons that are already reported in the literature for the removal

arsenite (As-III) are summarized in Table 4. Direct comparison of the adsorption capacities is very difficult due to different experimental conditions like pHs, temperatures, concentration ranges, adsorbent doses, and medium. Table 4 summarizes the sorption capacities of activated carbons from different sources calculated from the Langmuir isotherm model in an aqueous medium. It is evident that the adsorbent used in our case has the highest adsorption capacity of 4.63 mg/g for arsenite removal from aqueous solutions as compared to other adsorbents used [1,11,22,27,41].

3.4. Thermodynamics for the removal of arsenite onto Fe-GAC surfaces

Fig. 7 shows the effect of temperature on the removal of arsenite onto Fe-GAC. The results show that with the increase in temperature the removal efficiency of arsenite decreases, which is an indication of the exothermic nature of the adsorption process. Mondal et al. [42] has also reported the same type of observation for arsenate and arsenite removal with the suggestion that with the increase in temperature the mobility of ions will increase as a result surface precipitation

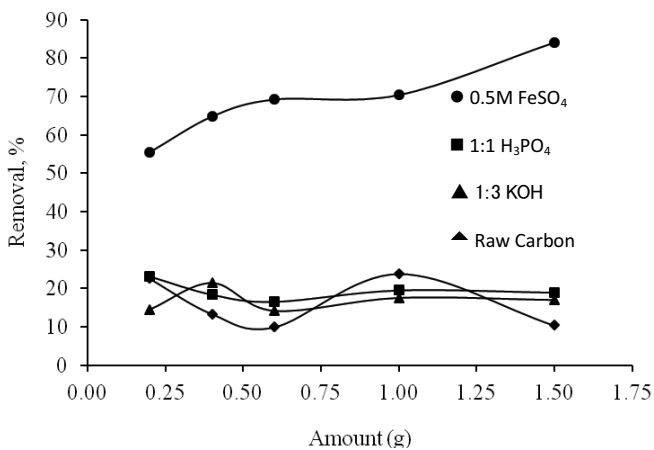


Fig. 3. % removal of arsenite using raw, 0.5 M FeSO_4 , H_3PO_4 and KOH.

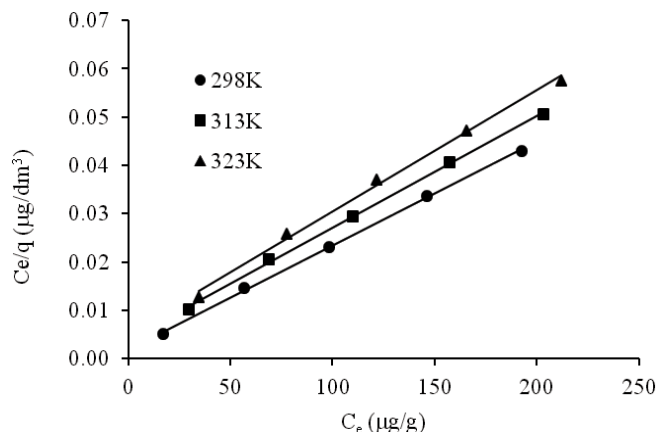


Fig. 4. Langmuir isotherms for the sorption of arsenite onto Fe-GAC at different temperatures.

Table 3
Isothermal parameters obtained for the adsorption of arsenite onto Fe-AC

| Isotherm model | Temperature/K | Estimated isotherm parameters | | | |
|-----------------|---------------|---------------------------------|---------------------------------|-------|---------------|
| | | X_m (mg/g) | b (dm^3/mg) | R^2 | R_L |
| Langmuir | 298 | 4.630 | 0.0085 | 0.999 | 0.0004–0.0011 |
| | 313 | 4.310 | 0.0165 | 0.999 | 0.0002–0.0005 |
| | 323 | 3.984 | 0.0213 | 0.996 | 0.0002–0.0006 |
| Freundlich | | K (mg/g) | $1/n$ | R^2 | |
| | 298 | 2.508 | 0.1108 | 0.991 | |
| | 313 | 1.679 | 0.1659 | 0.991 | |
| | 323 | 1.487 | 0.9847 | 0.985 | |
| Temkin isotherm | | A (dm^3/mg) | B | R^2 | |
| | 298 | 0.117 | 0.0023 | 0.990 | |
| | 313 | 0.369 | 0.0017 | 0.992 | |
| | 323 | 474 | 0.0018 | 0.973 | |

will decrease and also the stability of the bonds between the active sites of GAC and arsenic moiety decreases with the increase in temperature.

Sorption may occur as a result of two types of forces: enthalpy-related and entropy-related forces [43]. The enthalpy and entropy of the system were calculated from the Van't Hoff plots of $\ln K_D$ vs. $1/T$ for different temperatures of 298, 313 and 323 K, in which the slope of the plot is $-\Delta H^\circ/R$ and the intercept of the plot is $\Delta S^\circ/R$ (Fig. 8).

$$\ln K_D = -\frac{\Delta H^\circ}{RT} + \frac{\Delta S^\circ}{R} \tag{5}$$

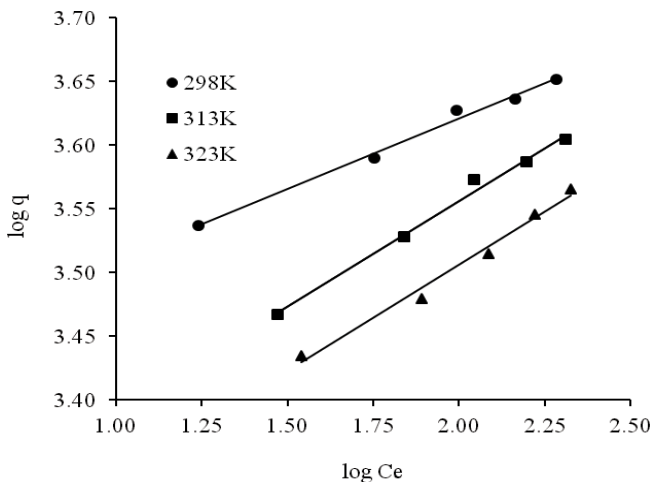


Fig. 5. Freundlich isotherms for the sorption of arsenite onto Fe-GAC at different temperatures.

where ΔH° and ΔS° are the enthalpy and entropy change respectively, R = gas constant (8.314 J/mol K), T = thermodynamic temperature (K).

Sorption of a chemical on a solid sorbent occurs when the free energy of the sorptive exchange is negative [43] and it can be calculated from the following equation:

$$\Delta G^\circ = \Delta H^\circ - T\Delta S^\circ \tag{6}$$

where ΔG° is the change of the Gibbs free energy (kJ/mol); ΔH° is the change in enthalpy (kJ/mol), and ΔS° is the change in entropy (kJ/mol K). ΔH° represents the difference in binding energies between the sorbent and the sorbate (solute) and between the solvent and the solute.

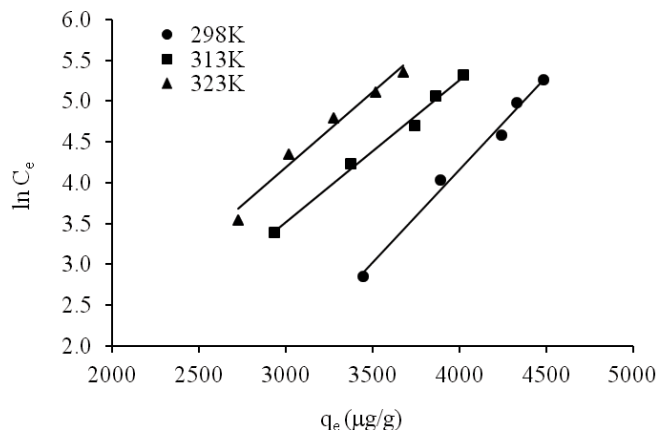


Fig. 6. Temkin isotherms for the sorption of arsenite onto Fe-GAC at different temperatures.

Table 4

Comparative evaluation of sorption capacity of arsenite (As-III) onto different types of activated carbon-based on Langmuir isotherm model from aqueous solution

| Adsorbent | pH | Concentration range | Surface area (m ² /g) | Temperature, K | Adsorption capacity (mg/g) | Reference |
|--|------|---------------------|----------------------------------|----------------|----------------------------|--------------|
| AC from pine cone coated with FeSO ₄ | 7.26 | 100 µg/L | – | 298 | 4.63 | Present work |
| AC from olive pulp and olive stone, carbon A | 7.0 | 5–20 mg/L | 1,030 | 298 | 1.393 | [11] |
| AC from olive pulp and olive stone, carbon B | 7.0 | 5–20 mg/L | 1,850 | 298 | 0.8555 | [11] |
| AC from olive pulp and olive stone, carbon C | 7.0 | 5–20 mg/L | 1,610 | 298 | 0.738 | [11] |
| AC from olive pulp and olive stone, carbon D | 7.0 | 5–20 mg/L | 732 | 298 | 0.210 | [11] |
| Pine wood char | 3.5 | 10–100 µg/L | 2.73 | 298 | 0.0012 | [22] |
| Oak wood char | 3.5 | 10–100 µg/L | 2.04 | 298 | 0.006 | |
| Oak bar char | 3.5 | 10–100 µg/L | 25.4 | 298 | 0.0074 | [22] |
| Pine bark char | 3.5 | 10–100 µg/L | 1.88 | 298 | 12 | [22] |
| Coaly AC | 3.7 | 5.0 mg/L | >1,000 | 303 | 0.026 | [1] |
| Activated carbon from rice hull | 4.5 | 1–10 mg/L | | 298 | 1.28 ± 0.03 | [41] |
| Activated carbon from areca nut | 4.5 | 1–10 mg/L | | 298 | 0.87 ± 0.04 | [41] |
| Manganese coated activated carbon from rice hull | 4.5 | 1–10 mg/L | | 298 | 1.52 ± 0.05 | [41] |
| Manganese coated activated carbon from areca nut | 4.5 | 1–10 mg/L | | 298 | 1.24 ± 0.04 | [41] |
| Activated carbon, RFe modified | 7–11 | 50 µg/L | 1,200 | 321 | 1.606 | [27] |

The thermodynamic parameters calculated according to Eqs. (5) and (6) are listed in Table 5. The negative values of ΔG° at all temperatures indicate the spontaneous nature of the adsorption of arsenite onto Fe-GAC surfaces. Moreover, the negative values of Gibbs free energy change indicate that all the solutes are favored to stay in the stationary phase rather than in the mobile phase. The solute transfer from the mobile to the stationary phase is enthalpically favorable (negative value) and entropically unfavorable (negative value), and the enthalpic contribution is predominant compared to the entropic contribution. The negative values of entropy change (ΔS°) correspond to a decrease in the degree of freedom of the adsorbed species while the negative values of the change in enthalpy indicate that the adsorption is physical in nature involving weak forces of attraction and is also exothermic, thereby demonstrating that the process is stable energetically.

3.5. Adsorption kinetic

The time-dependent adsorption behavior was measured by varying the equilibrium time between adsorbate and adsorbent in the range of 5–120 min. The percentage adsorption of arsenite as a function of contact time indicates that the equilibrium between the arsenite and Fe-GAC was attained within 60 min (Fig. 9).

Pseudo-first-order and pseudo-second-order kinetic model was applied to the arsenite sorption onto Fe-GAC. First, the

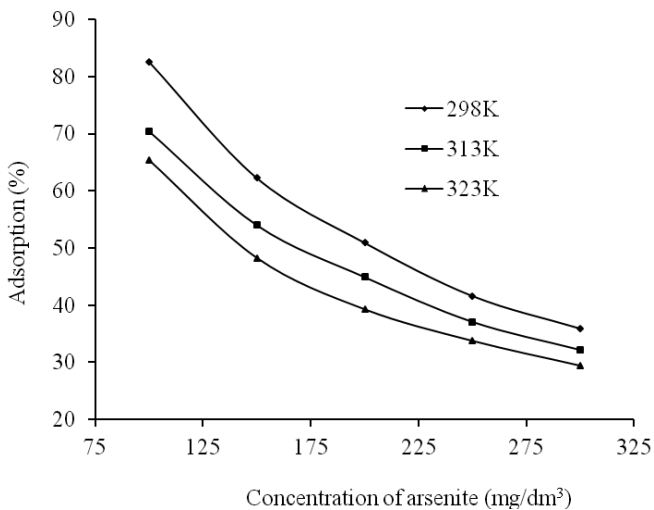


Fig. 7. Effect of temperature of the adsorption of arsenite onto Fe-GAC at different temperatures.

Table 5

Thermodynamic parameters for the adsorption of arsenite onto Fe-GAC

| Concentration of arsenite ($\mu\text{g}/\text{dm}^3$) | $-\Delta H^\circ$ (kJ/mol) | $-\Delta S^\circ$ (kJ/K mol) | $-\Delta G^\circ$ (KJ/mol) | | |
|---|----------------------------|------------------------------|----------------------------|--------|-------|
| | | | 298 K | 313 K | 323 K |
| 150 | 18.167 | 25.770 | 10.048 | 10.101 | 9.843 |
| 200 | 14.841 | 18.390 | 9.361 | 9.085 | 8.901 |
| 250 | 10.580 | 7.287 | 8.408 | 8.299 | 8.226 |
| 300 | 9.321 | 5.067 | 7.811 | 7.735 | 7.684 |

kinetics of sorption was analyzed by the pseudo-first-order equation given by Lagergren [45] as,

$$\log(q_e - q_t) = \log q_e - \left(\frac{k_1}{2.303}\right)t \quad (7)$$

where q_e and q_t are the amounts of solute adsorbed per gram at equilibrium and at time t (min), respectively, and k_1 (/min)

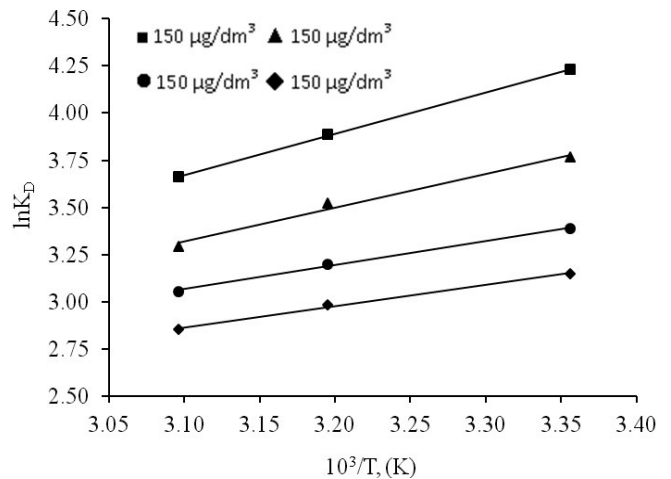


Fig. 8. Van't Hoff plots for the sorption of arsenite onto Fe-GAC at different concentrations.

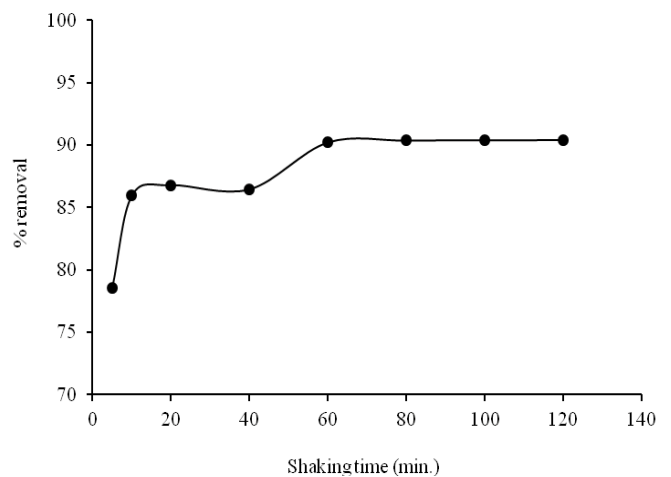


Fig. 9. Effect of shaking time on the sorption of arsenite onto Fe-GAC.

is the rate constant for adsorption. Values of k_1 and q_e were calculated from the slope and intercept of the plot of $\log(q_e - q_t)$ vs. t (Fig. 10).

The pseudo-second-order rate expression was used to describe chemisorption involving valence forces through the sharing or exchange of electrons between the adsorbent and adsorbate as covalent forces. The advantage of using this model is that there is no need to know the equilibrium capacity from the experiments, as it can be calculated from the model. In addition, the initial adsorption rate can also be obtained from the model. The rate of pseudo-second-order reaction may be dependent on the amount of solute sorbed on the surface of the adsorbent and the amount sorbed at equilibrium. The pseudo-second-order kinetic model [46] is expressed as:

$$\frac{t}{q_t} = \left(\frac{1}{k_2 q_e^2} \right) + \left(\frac{1}{q_e} \right) t \tag{8}$$

where k_2 (g/mg min) is the rate constant of second-order adsorbent. The values of q_e and k_2 were calculated from the slope and intercept of the linear plot of t/q_t vs. t respectively (Fig. 11). The initial sorption rate (h) was calculated from the following relation:

$$h = k_2 q_e^2 \tag{9}$$

where h is the initial sorption rate (mg/g min).

The validity of the kinetic models is tested by the magnitude of the regression coefficient R^2 , given in Table 6. The R^2 value obtained for pseudo-first-order kinetics was 0.617. In contrast, the application of a pseudo-second-order model leads to a much better regression coefficient ($R^2 = 0.999$). Table 6 provides pseudo-first-order rate constants k_1 , and pseudo-second-order rate constants k_2 , h .

3.6. Competitive sorption of arsenite in the presence of other heavy metal ions

Compared to the literature for arsenite adsorption alone, relatively few data are available for the multi-component metal ions adsorption. It has been reported in the literature

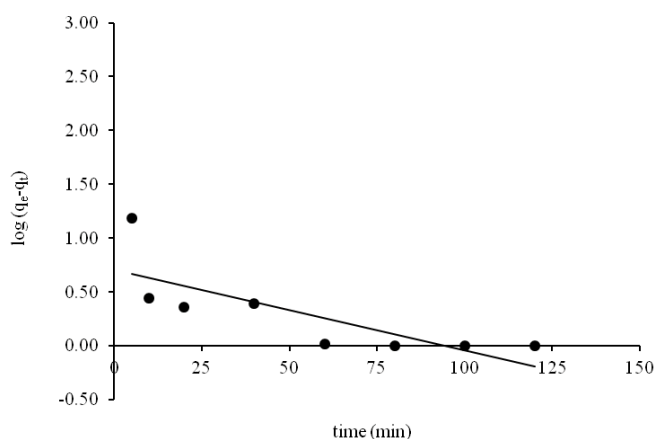


Fig. 10. Pseudo-first-order rate plot for arsenite onto Fe-GAC.

that generally the sorption capacity for metals increased or decreased when more than one metal ion is present in the solution. The sorption of arsenite in the presence of various metal ions by varying the amount of Fe-GAC (0.2–1.5 g) is shown in Fig. 12. The result shows maximum removal efficiency for selenium (>90%) followed by arsenic (>80%) by using 1.2 g of adsorbent. However, the other studied metal ions have shown no significant removal efficiency onto Fe-GAC. Also, these added metal ions have shown no significant effect on the reduction of sorption capacity of arsenite when present in the solution at the same concentration level. The sorption of other metals onto Fe-GAC was negligible and found to be less than 30% as compared to arsenic and selenium. This may be due to the fact that arsenite has a higher affinity for the sorption sites of Fe-GAC as compared to other metal ions except for selenium. This may be due to the fact that metal with higher electronegativity will show a higher adsorption capacity [47]. Also, the adsorption of heavy metal with a larger ionic radius is greater than those with a smaller radius [48]. The electronegativity of selenium and arsenic is 2.55 and 2.18 respectively, while its ionic radius is 64 and 58 respectively. Selenium having higher electronegativity and ionic radius shows greater adsorption capacity than arsenic and other metals in the solution.

3.7. Point of zero charges, effect of pH and mechanism for arsenite sorption onto Fe-GAC

The pH at which the sorbent surface charge takes a zero value is defined as the point of zero charges (pHpzc). At this

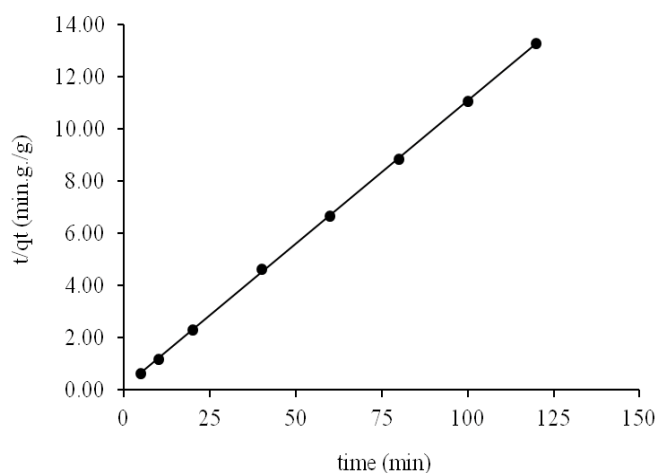


Fig. 11. Pseudo-second-order rate plot for arsenite onto Fe-GAC.

Table 6
Comparison of the pseudo-first-order and pseudo-second-order model for arsenite sorption onto Fe-GAC

| Kinetic rate equation | Estimated kinetic parameters | | |
|------------------------------|------------------------------|--------------------|-------|
| Pseudo-first-order kinetics | k_1 (min) | $q_{e,exp}$ (mg/g) | R^2 |
| | 0.0173 | 5.07 | 0.617 |
| Pseudo-second-order kinetics | k_2 (g/mg/min) | h (mg/g/min) | R^2 |
| | 0.1094 | 9.11 | 0.999 |

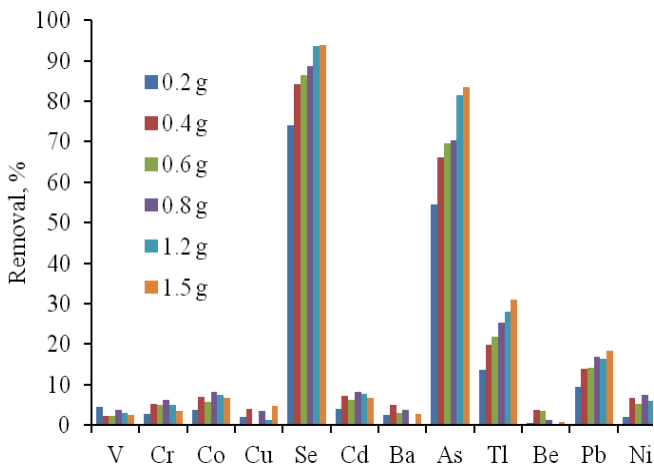


Fig. 12. Sorption of arsenite in the presence of various metal ions.

pH, the charge of the positive surface sites is equal to that of the negative ones. The pH_{pzc} was calculated from the plot of change in solution pH (ΔpH) vs. initial pH (pH_i) [49] which shows that with increasing initial solution pH, the pH change became more negative and the zero value of ΔpH was reached at pH_i value of 2.5, which is considered as the pH_{pzc} of the Fe-GAC (activated carbon with 0.5 M $FeSO_4$). It has been reported that at pH values of solution higher than pH_{pzc} , the sorbent surface is negatively charged and could better interact with metal positive species while at pH values lower than pH_{pzc} , the solid surface is positively charged and could interact with negative species [50].

pH is one of the most important parameters that have a significant role in the removal of arsenite by sorption. Fig. 13 shows that the adsorption of arsenite increase from 9.7% to 99.8% as the pH of the solution increased from 2.6 to 7.2. The maximum adsorption occurs at a pH of 7.2 (99.8%), followed by a decrease in sorption as the pH increases from 7.2 to 12.4. Having a pH_{pzc} of 2.5 clearly indicates that the surface of the Fe-GAC is predominantly negatively charged under the experimental pH range (2.6–12.4).

Various mechanisms have been reported for the sorption of arsenite including van der waals force between arsenite and GAC [1], the formation of inner and outer-sphere complexes onto amorphous Fe oxide and outer-sphere complexes onto amorphous Al oxid. Payne and Abdel-Fattah [27] suggested that ferric arsenite was produced and the mechanism for the removal of arsenic was adsorption on iron-modified adsorbents, which refers to the formation of surface complexes between soluble arsenic species and the surface hydroxyl groups, as arsenic gets into contact with the iron sites. Goldberg and Johnston et al. [51] proposed the mechanism of arsenic removal as the hybrid material was governed by electrostatic attraction and complexation between the positively charged surface hydroxyl group and arsenite. Mondal et al. [42] reported that GAC contains oxides of aluminum, calcium, and silicon, those are responsible for the development of charges on the adsorbent surface when GAC comes in contact with water. At lower pH, the As(III) species is present in non-ionic form but GAC surface is positively charged and at higher pH As(III) is negatively charged but the positive charge intensity onto

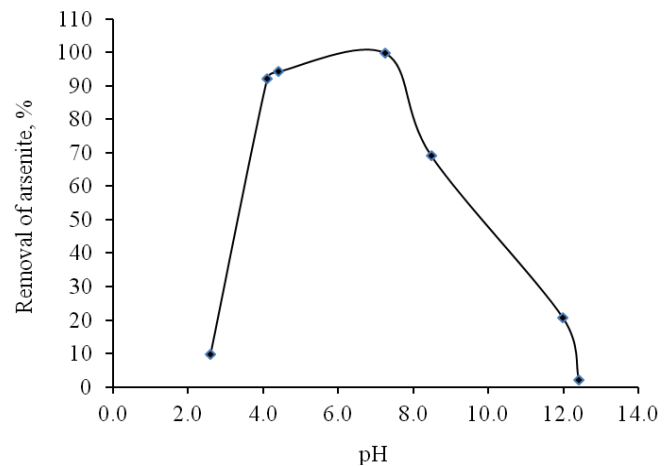
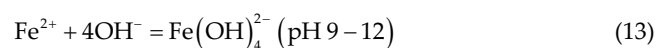
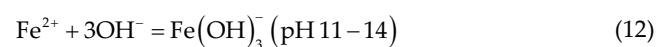
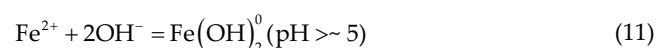
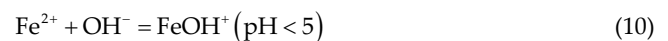


Fig. 13. Effect of pH on the removal of arsenite onto Fe-GAC.

the GAC surface is reduced. As(III) although the negative charge increases with the increase of pH the GAC surface also reduces positive nature, hence, the As(III) removal is also reduced at higher pH. Several factors such as pH of the solution, type of adsorbent used, activation process, surface functional groups available for coordination and other factors are involved in the sorption mechanism of arsenite.

Our results were also in agreement with the previous findings where the adsorption of arsenite was highly dependent on pH of the solution. Redox potential (Eh) and pH are the most important factors controlling arsenic and iron speciation in water. Arsenite is usually present as H_3AsO_3 at $pH < 9$, and as $H_2AsO_3^-$ at pH greater than 9 in water [52]. Analysis of Eh-pH diagram for Fe^{2+} results in the following species at different pH:



In our experiments, the maximum removal of arsenite was observed at $pH \sim 7.0-7.2$. At this pH H_3AsO_3 being the dominant species of arsenite in aqueous solutions forms strong inner-sphere complexes with GAC-FeOH as follows:



With continuously increasing pH and OH⁻ quantity at pH > 8, the negative charge of ferrous hydroxide increased (Eqs. (15) and (16)), and the repel function to HAsO₃⁻ and HAsO₂²⁻ was enhanced resulting in the decline in the removal efficiency of arsenite at higher pH.

4. Conclusion

The present study shows that the activated carbon produced from the cones of *Pinus roxburghii* and its further chemical activation with FeSO₄ proves to be an effective adsorbent for the removal of arsenite from aqueous solutions. In batch studies, the adsorption was dependent on initial arsenite concentration, pH, adsorbent dosage, and temperature. The pseudo-second-order chemical reaction kinetics provide the best correlation of the data ($R^2 > 0.99$). The adsorption capacity decreased with increasing temperature. The sorption process is found to be exothermic in nature with a negative value of entropy, ΔS° . The negative value of Gibbs free energy, ΔG° indicates that the adsorption occurs via a spontaneous process. H₃AsO₃ being the dominant species of arsenite at pH 7.2 is responsible for adsorption onto negatively charged Fe-GAC surfaces through inner-sphere complexation. Fe-GAC shows the highest sorption efficiency for arsenite (>83%) in the presence of V, Cr, Co, Cu, Cd, Ba, Tl, Be, Pb and Ni which were found to be less than 30%. Thus, when employing iron preloading activated carbon, approximately 99% of arsenite was successfully removed from aqueous solutions. Langmuir Isotherms which were the best fit in our studies reveal that this sorbent is quite favorable when compared with other activated carbons prepared from different materials both in its maximum adsorption capacity and removal rate.

Acknowledgments

The author is thankful to the Council for International Exchange of Scholars (CIES), Institute of International Education (IIE), Washington, DC for providing financial support and sponsoring this research work under Fulbright Visiting Research Scholar Program.

References

- [1] Y. Wu, X. Ma, M. Feng, M. Liu, Behavior of chromium and arsenic on activated carbon, *J. Hazard. Mater.*, 159 (2008) 380–384.
- [2] T. Levine, W. Marcus, C. Chen, A. Rispin, Special Report on Ingested Inorganic Arsenic Skin Cancer, Nutritional Essentiality, Risk Assessment Forum, U.S. Environmental Protection Agency, EPA-625/3-87/013, Washington, D.C., 20460, 1988.
- [3] Agency for Toxic Substances and Disease Registry (ATSDR), Toxicological Profile for Arsenic, U.S. Department of Health and Human Services, Public Health Service, Atlanta, GA, 2007.
- [4] United States Environmental Protection Agency, Arsenic and Clarifications to Compliance and New Source Monitoring Rule 66 FR 6976, Office of Water (66 FR 6976), 2001, EPA 816-F-01-004.
- [5] World Health Organization, Guidelines for Drinking Water Quality: Recommendations, Geneva, 1, 1993.
- [6] S.K. Tiwari, V.K. Pandey, Removal of arsenic from drinking water by precipitation and adsorption or cementation: an environmental prospective, *Recent Res. Sci. Technol.*, 5 (2013) 88–91.
- [7] Y. Sato, M. Kang, T. Kamei, Y. Magara, Performance of nanofiltration for arsenic removal, *Water Res.*, 36 (2002) 3371–3377.
- [8] G. Ghurye, D. Clifford, Laboratory Study on the Oxidation of Arsenic III to Arsenic V, EPA/600/R-01/021, March 2001, p. 87.
- [9] USEPA, Technologies, and Costs for Removal of Arsenic from Drinking Water (EPA 815-R-00-028), United States Environmental Protection Agency, Washington, D.C., 2000.
- [10] K.S. Ng, Z. Ujang, P. Le-Clech, Arsenic removal technologies for drinking water treatment, *Rev. Environ. Sci. Biotechnol.*, 3 (2004) 43–53.
- [11] T. Budinova, N. Petrov, M. Razvigorova, J. Parra, P. Galiatsatou, Removal of arsenic(III) from aqueous solution by activated carbons prepared from solvent extracted olive pulp and olive stones, *Ind. Eng. Chem. Res.*, 45 (2006) 1896–1901.
- [12] G.N. Manju, C. Raji, T.S. Anirudhan, Evaluation of coconut husk carbon for the removal of arsenic from water, *Water Res.*, 32 (1998) 3062–3070.
- [13] J. Laine, A. Calafat, M. Labady, Preparation and characterization of activated carbons from coconut shell impregnated with phosphoric acid, *Carbon*, 27 (1989) 191–195.
- [14] D. Mohan, K.P. Singh, S. Singh, D. Ghosh, Removal of α -picoline, β -picoline, and γ -picoline from synthetic wastewater using low cost activated carbons derived from coconut shell fibers, *Environ. Sci. Technol.*, 39 (2005) 5076–5086.
- [15] D. Mohan, K.P. Singh, S. Singh, D. Ghosh, Removal of pyridine derivatives from aqueous solution by activated carbons developed from agricultural waste materials, *Carbon*, 43 (2005) 1680–1693.
- [16] D. Mohan, K.P. Singh, V.K. Singh, Trivalent chromium removal from wastewater using low cost activated carbon derived from agricultural waste material and activated carbon fabric cloth, *J. Hazard. Mater.*, 135 (2006) 280–295.
- [17] F.M.C. Alvim, Preparation of activated carbon for air pollution control, *Fuel*, 67 (1988) 1237–1241.
- [18] C.A. Toles, W.E. Marshall, M.M. Johns, Granular activated carbon from nutshells for the uptake of metals and organic compounds, *Carbon*, 35 (1997) 1407–1414.
- [19] C.L. Chuang, M. Fan, M. Xu, R.C. Brown, S. Sung, B. Saha, C.P. Huang, Adsorption of arsenic (V) by activated carbon prepared from oat hulls, *Chemosphere*, 61 (2005) 478–483.
- [20] M.R. Samarghandi, M. Hadi, S. Moayedi, F.B. Askari, Two-parameter isotherms of methyl orange sorption by pinecone derived activated carbon, *Iran. J. Environ. Health Sci. Eng.*, 6 (2009) 285–294.
- [21] S. Dawood, K.S. Tushar, C. Phan, Synthesis and characterization of novel-activated carbon from waste biomass pine cone and its application in the removal of congo red dye from aqueous solution by adsorption, *Water Air Soil Pollut.*, 225 (2013) 1818.
- [22] M. Momcilovic, M. Purenovic, A. Bojic, A. Zarubica, M. Randelovic, Removal of lead(II) ions from aqueous solutions by adsorption onto pine cone activated carbon, *Desalination*, 276 (2011) 53–59.
- [23] U. Gecgel, H. Kolancilar, Adsorption of Remazol Brilliant Blue R on activated carbon prepared from a pine cone, *Nat. Prod. Res.*, 26 (2012) 659–664.
- [24] M.Z. Momcilovic, A.E. Onjia, M.M. Purenovic, A.R. Zarubica, M.S. Randelovic, Removal of a cationic dye from water by activated pinecones, *J. Serb. Chem. Soc.*, 77 (2012) 761–774.
- [25] G. Duman, Y. Onal, C. Okutucu, S. Onenc, J. Yanik, Production of activated carbon from pine cone and evaluation of its physical, chemical, and adsorption properties, *Energy Fuels*, 23 (2009) 2197–2204.
- [26] N.V. Vinh, M. Zafar, S.K. Behera, H.S. Park, Arsenic(III) removal from aqueous solution by raw and zinc-loaded pine cone biochar: equilibrium, kinetics, and thermodynamics studies, *Int. J. Environ. Sci. Technol.*, 12 (2015) 1283–1294.
- [27] K.B. Payne, T.M. Abdel-Fattah, Adsorption of arsenate and arsenite by iron-treated activated carbon and zeolites: effects of pH, temperature, and ionic strength, *J. Environ. Sci. Health*, 40 (2005) 723–749.
- [28] G.P. Gillman, E.A. Sumpter, Modification to the compulsive exchange method for measuring exchange characteristics of soils, *Aust. J. Soil Res.*, 24 (1986) 61–66.
- [29] R.M. Shrestha, A.P. Yadav, B.P. Pokharel, R.R. Pradhananga, Preparation and characterization of activated carbon from

- Lapsi (*Choerospondias axillaris*) seed stone by chemical activation with phosphoric acid, Res. J. Chem. Sci., 2 (2012) 80–86.
- [30] G.W. Sears, Determination of specific surface area of colloidal silica by titration with sodium hydroxide, Anal. Chem., 28 (1956) 1981–1983.
- [31] S.S. Tahir, N. Rauf, Removal of a cationic dye from aqueous solutions by adsorption onto bentonite clay, Chemosphere, 63 (2006) 1842–1848.
- [32] R. Helleur, N. Popovic, M. Ikura, M. Stanciulescu, D. Liu, Characterisation and potential application of pyrolytic char from ablative pyrolysis of used tyres, J. Anal. Appl. Pyrolysis, 58–59 (2001) 813–824.
- [33] E.C. Bernardo, R. Egashira, J. Kawasaki, Decolorization of molasses' wastewater using activated carbon prepared from cane bagasse, Carbon, 35 (1997) 1217–1221.
- [34] R. Baccar, J. Bouzida, M. Feki, A. Montiel, Preparation of activated carbon from Tunisian olive-waste cakes and its application for adsorption of heavy metal ions, J. Hazard. Mater., 162 (2009) 1522–1529.
- [35] Association Scientifique et Technique pour l'Eau et l'Environnement (ASTEE), Réglementation et traitement des eaux destinés à la consommation humaine, 1ère édition, Paris, 2006.
- [36] I. Langmuir, The constitution and fundamental properties of solids and liquids, J. Am. Chem. Soc., 38 (1916) 2221–2295.
- [37] E. Zeynep, N. A. Filiz, Equilibrium and kinetic mechanism for reactive black 5 sorption onto high lime soda fly ash, J. Hazard. Mater., 143 (2007) 226–232.
- [38] H.M.F. Freundlich, Über die adsorption in losungen, Zeitschrift für Physikalische Chemie, 57 (1906) 385–470.
- [39] M.J. Temkin, V. Pyzhev, Recent modifications to Langmuir isotherms, Acta Phys. URSS, 12 (1940) 217–222.
- [40] R. Palas, K.M. Naba, B. Shreya, D. Biswajit, D. Kousik, Removal of arsenic (III) and arsenic (V) on chemically modified low-cost adsorbent: batch and column operations, Appl. Water Sci., 3 (2013) 293–309.
- [41] Lalmunsiana, D. Tiwari, S.-M. Lee, Activated carbon and manganese coated activated carbon precursor to dead biomass in the remediation of arsenic contaminated water, Environ. Eng. Res. 17 (2012) S41–S48.
- [42] P. Mondal, C. Balomajumder, B. Mohanty, A laboratory study for the treatment of arsenic, iron, and manganese bearing ground water using Fe³⁺ impregnated activated carbon: effects of shaking time, pH and temperature, J. Hazard. Mater., 144 (2007) 420–426.
- [43] T.E.M. ten Hulscher, G. Cornelissen, Effect of temperature on sorption equilibrium and sorption kinetics of organic micro-pollutants – a review, Chemosphere, 32 (1996) 609–626.
- [44] S. Senthilkumar, P. Kalaamani, K. Porkodi, P.R. Varadarajan, C.V. Subburaam, Adsorption of dissolved reactive red dye from aqueous phase onto activated carbon prepared from agricultural waste, Bioresour. Technol., 97 (2006) 1618–1625.
- [45] S. Lagergren, Zur theorie der sogenannten adsorption gelöster stoffe, Kungliga Svenska Vetenskapsakademiens, Handlingar, 24 (1898) 1–39.
- [46] Y.S. Ho, G. McKay, Pseudo-second-order model for sorption processes, Process Biochem., 34 (1999) 451–465.
- [47] V.C. Taty-Costodes, H. Fauduet, C. Porte, A. Delacroix, Removal of Cd(II) and Pb(II) ions, from aqueous solutions, by adsorption onto sawdust of *Pinus sylvestris*, J. Hazard. Mater., 105 (2003) 121–42.
- [48] A.P. Olalekan, A.O. Dada, A.O. Okewale, Comparative adsorption isotherm study of the removal of Pb²⁺ and Zn²⁺ onto agricultural waste, Res. J. Chem. Environ. Sci., 1 (2013) 22–27.
- [49] E.O. Augustine, Y.S. Ho, Effect of temperatures and pH on methyl violet biosorption by *Mansonia* wood sawdust, Bioresour. Technol., 99 (2008) 5411–5417.
- [50] B. Radomir, J.M. Ljupković, R. Miljana, K. Miloš, B. Danijela, M.S. Dragana-Linda, L.B. Aleksandar, Removal Cu(II) ions from water using sulphuric acid treated *Lagenaria vulgaris* shell (*Cucurbitaceae*), Biol. Nyssana, 2 (2011) 85–89.
- [51] S. Goldberg, C.T. Johnston, Mechanisms of arsenic adsorption on amorphous oxides evaluated using macroscopic measurements, vibrational spectroscopy, and surface complexation modeling, J. Colloid Interface Sci., 234 (2001) 204–216.
- [52] D.G. Brookins, Eh-pH Diagrams for Geochemistry, Springer-Verlag, New York, 1988, p. 176.